Т. 88, № 2 **ЖУРНАЛ ПРИКЛАДНОЙ СПЕКТРОСКОПИИ** МАРТ — АПРЕЛЬ 2021
V. 88, N 2 **JOURNAL OF APPLIED SPECTROSCOPY** MARCH — APRIL 2021

APPLICATION OF ^{1}H LOW-FIELD NMR SPECTROSCOPY FOR THE DETERMINATION OF THE CONCENTRATION AND MOLECULE WEIGHT OF POLYCARBOXYLATE SUPERPLASTICIZERS

Y. Ji *, **Zh. Sun** *, **M. Pang, J. Yang**

Key Laboratory of Advanced Civil Engineering Materials, Ministry of Education,
School of Materials Science and Engineering at Tongji University,
Shanghai 201804, China; e-mail: tjyanliangji@tongji.edu.cn, sunzhptongji@163.com

As a type of water reducer, polycarboxylate superplasticizers (PCEs) has been widely used in the concrete industry. The concentration and molecule weight of PCEs have a profound impact on the performance of fresh concrete. Based on ^{1}H low-field nuclear magnetic resonance (NMR) spectroscopy, this paper developed a novel method for the determination of the concentration and characterization of the molecule weight of PCEs. Five types of PCEs with various ether to acid ratios (3:1 to 5:1) and functional groups were synthetized in laboratory conditions, and their molecular structures were characterized by size exclusion chromatography. PCE solutions with concentrations from 0 to 40% were measured using the Carr–Purcell–Meiboom–Gill sequence by ^{1}H low-field NMR. The results showed that the T_2 value of the main peak has a linear relation with the PCE concentration. The signal intensity of peaks whose T_2 values are smaller than 10 ms of the PCE solutions with a concentration of 20% is linearly correlated to the molecule weight of PCEs.

Keywords: *polycarboxylate superplasticizers, concentration, molecule weight, ^{1}H low-field Carr–Purcell–Meiboom–Gill spectroscopy.*

ПРИМЕНЕНИЕ НИЗКОПОЛЕВОЙ ^{1}H ЯМР-СПЕКТРОСКОПИИ ДЛЯ ОПРЕДЕЛЕНИЯ КОНЦЕНТРАЦИИ И МОЛЕКУЛЯРНОЙ МАССЫ ПОЛИКАРБОКСИЛАТНЫХ СУПЕРПЛАСТИФИКАТОРОВ

Y. Ji *, **Zh. Sun** *, **M. Pang, J. Yang**

УДК 539.143.43

Школа материаловедения и инженерии Университета Тунцзи,
201804, Шанхай, Китай; e-mail: tjyanliangji@tongji.edu.cn, sunzhptongji@163.com

(Поступила 8 января 2020)

На основе низкополевой спектроскопии ядерного магнитного резонанса (ЯМР) ^{1}H разработан метод определения концентрации и молекулярной массы поликарбоксилатных суперпластификаторов (PCE). Синтезированы пять типов PCE с различными отношением эфира к кислоте (от 3:1 до 5:1) и функциональными группами, молекулярные структуры разных PCE охарактеризованы с помощью эксклюзионной хроматографии. Растворы PCE с концентрацией 0–40 % изучены с помощью последовательности Карра—Парселла—Мейбума—Гилла методом низкополевой ^{1}H ЯМР-спектроскопии. Результаты показывают, что значение T_2 основного пика линейно зависит от концентрации PCE. Интенсивность сигнала с $T_2 < 10$ мс для растворов PCE с концентрацией 20 % линейно коррелирует с молекулярной массой PCE.

Ключевые слова: *поликарбоксилатные суперпластификаторы, концентрация, молекулярная масса, низкополевая ^{1}H ЯМР-спектроскопия.*

Introduction. The addition of a water reducer can significantly increase fluidity (or workability) and lead to the higher mechanical strength and durability of concrete [1]. As the third generation of water reducers, polycarboxylate superplasticizers (PCEs) are used for ultra-high building and for the long-distance transportation of concrete [2, 3]. It is a known fact that the development of modern concrete engineering is inseparable from the help of polycarboxylate (PCE) superplasticizers.

PCEs can increase the fluidity of concrete in the early stage due to multiple effects, known as electrical repulsion and steric hindrance [3, 4]. Due to the effect of electrical repulsion, PCE superplasticizers cause the cement particles to be mutually exclusive. As a result, the dispersion is enhanced, and the mobility between the cement particles is promoted [5–7]. Besides, the side chains of PCE molecules point to the pore water, which may reduce the possibility of the formation of a flocculated structure by the cement particles (named as the effect of steric hindrance) [7]. The impacts of PCEs are all due to the fact that enough PCEs could be attached on the cement particles. In general, the concentration and molecule weight of PCEs have shown high relevance with the workability of concrete [8, 9]. However, the concentration of PCEs is generally not stable. Different synthetizing processes, such as water used in the raw materials, alter the concentration of PCEs as well as the molecule weight [1, 10]. In addition, the air-exchanging degree of the synthetizing and storage equipment will induce the evaporation on the PCEs surface, so the PCEs concentration will be influenced. Besides, it is not rare that producers intentionally dilute PCEs products in order to lower the product cost or due to the solubility of other chemical admixtures (i.e., retarders, air-entraining admixtures, and early strength admixtures). Therefore, rapid measurement of the concentration is essential to the application of PCEs, and the objective characterization of the molecule weight can provide guidelines for the design of the PCEs structure.

As a nondestructive method, ^{1}H low-field NMR has been widely used for various studies, i.e., water migration in pores [11], determination of the pore structure [12], as well as the determination of water populations in shale [13]. The sensitivity of ^{1}H low-field NMR to different forms of water molecules and water distribution in different porous materials may provide an alternative method for measuring both the PCE concentration and the weight of the molecules. In this study, five types of PCEs with various ether to acid ratios from 3:1 to 5:1 and functional groups (AM and AMPS) were synthesized in laboratory conditions, and their molecular structures were characterized by size exclusion chromatography (SEC). PCE solutions with concentrations from 0 to 40% were measured using the Carr-Purcell-Meiboom-Gill (CPMG) sequence by the NMR method. The relationship between NMR spectroscopy (expressed as T_2 relaxation time or signal intensity) and concentration, as well as molecule weight, is analyzed and discussed in this paper.

Experimental. The macro-monomer was industrial-grade methyl allyl polyethenoxy ether (HPEG, MW 2400 g/mol), manufactured by Dong Da Chemical Company. Analytical grades of acrylic acid (AA), 2-acrylamide-2-methylpropanesulfonic (AMPS), acrylamide (AM), hydrogen peroxide (H_2O_2), ammonium persulfate (APS), L-ascorbic acid, as well as 2-mercaptoacetic acid (TGA), were also used, purchased from Sinopharm Chemical Reagent Co., Ltd. Hydrogen peroxide was used as an oxidant and reductant. L-ascorbic acid and ammonium persulfate were used as initiators to decrease the initiating temperature. TGA was used as the chain transfer agent. The water used in this study was deionized.

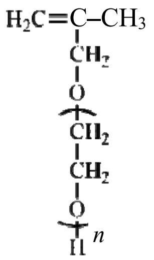

HPEG

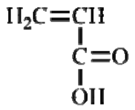

AA

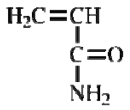

AM

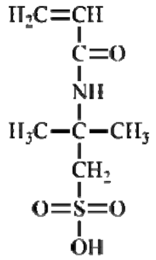

AMPS

The synthesis of PCEs can be described as follows. First, AA or other monomers (for their proportions, see Table 1) were mixed with a certain amount of water to prepare solution A (with a mass concentration of 53.3%). Considering the low dissolving ability, AMPS powders were mixed with a certain amount of water at first, and then the pre-prepared solution was mixed with the rest of the water and AA. L-ascorbic acid (0.15 g) and TGA (0.35 g) were mixed with water to prepare solution B with a mass concentration of 2.5% (the quantity of solution B was 20 g). HPEG was mixed with water to prepare solution C with a mass concentration of 56%. Then, we put solution C, hydrogen peroxide (1 g), and ammonium persulfate (2.2 g) into a glass reactor; then the reactor was kept at 60±0.5°C (2 h) in a water bath system. Peristaltic pumps were used to titrate solutions A and B into the synthesis system in the reactor gradually and uniformly for 3 h to complete the polymerization. During the titration, the whole system was mixed with an electric blender at a stirring speed of 55 r/min. After that, the copolymers were cooled down to 28°C, and then the NaOH (30%)

solution was gradually added until the pH of the copolymers reached 6–7. Finally, the unreacted monomers were removed from the synthesized polymers by the method according to the [6, 14].

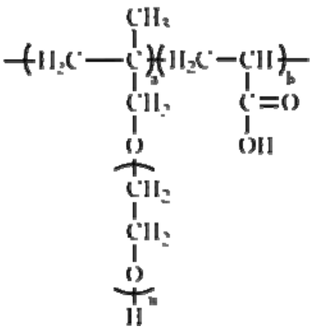

PCEs(HPEG-co-AA)

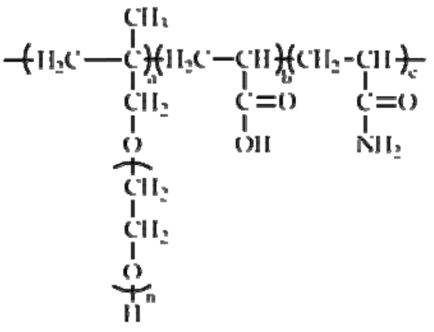

PCEs(HPEG-co-AA-CO-AM)

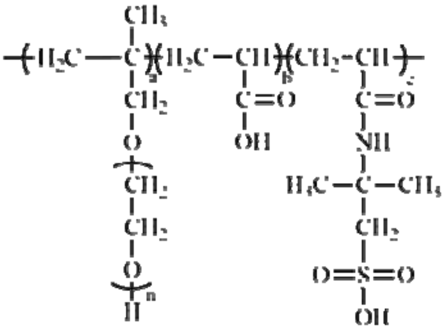

PCEs(HPEG-co-AA-CO-AMPS)

To gain information about the size of the synthesized PCEs, the size SEC, equipped with a refractive index detector and a multi-angle laser light scattering detector, was applied in this study. The weight average molecular weight (M_w), number average molecular weight (M_n), and polydispersity index (PDI = M_w/M_n) of the synthesized PCEs are summarized in Table 1.

TABLE 1. Molar Ratios of Monomers and Molecular Weight Determined by SEC of the Synthesized PCEs

PCEs types	AA	HPEG	AM	AMPS	Properties		
					M_n	M_w	PDI
AA3	3	1	–	–	81308	125215	1.54
AA4	4	1	–	–	124134	181235	1.46
AA5	5	1	–	–	126805	205424	1.62
AA2-AM	2	1	1	–	87342	138874	1.59
AA2-AMPS	2	1	–	1	126894	189072	1.49

^{1}H Low-field NMR. The NMR instrument (PQ-001; Niumag Electric Corporation, Shang Hai, China) used in this study has a 25 mm RF coil, and its magnetic field is 0.50 T. To keep the stability, the magnet was stored in constant temperature conditions (32°C). The decay curves for the ^{1}H proton of the sample was measured using the CPMG sequence, and the parameters including the echo time ($\tau_1 = 0.30$ ms), echo numbers (NECH = 15000), and number of scans (NS = 4) were kept constant throughout the NMR measurements. The inverse Laplace transform algorithm [14, 15] was used to fit the transverse relaxation decay curve to obtain the T_2 relaxation time.

The nuclei (^{1}H) of water molecules in voids are moving randomly because of Brownian motion during the NMR experiment [16, 17]. Thus, the T_2 relaxation time and the signal intensity of a sample can reflect the structure. The T_2 relaxation of water in the pores of a material can be thus related to the pore (or space) size [17–19]:

$$1/T_2 = 1/T_{\text{bulk}} + \rho_2 S/V\,, \tag{1}$$

where ρ_2 is the so-called surface relaxivity for the T_2 relaxation, and S and V stand for the surface area and volume of the pores, respectively. As T_{bulk} is in general quite large in comparison to the surface relaxation, the first term can be neglected [14, 20]. Hence the T_2 relaxation time can provide information on the V/S, which is proportional to the pore size.

Results and discussion. *T_2 distribution of the PCEs-water solution.* In order to compare the impacts of the PCE concentration on the transverse relaxation time (T_2) distribution, first we calculated the solid weight concentration of the PCEs solution (taking the loss from the unreacted monomers into consideration), then titrated the solutions with water until it reached a concentration of 40% (±0.2%). Thereafter we gradually added water to prepare PCEs-water solutions with concentrations from 0 to 40%. The PCEs samples (7.5 g) were then measured by ^{1}H low-field NMR with the CPMG sequence. The results concerning the transverse relaxation time (T_2) distribution of PCEs-water solutions (PCEs-AA5) are shown in Fig. 1.

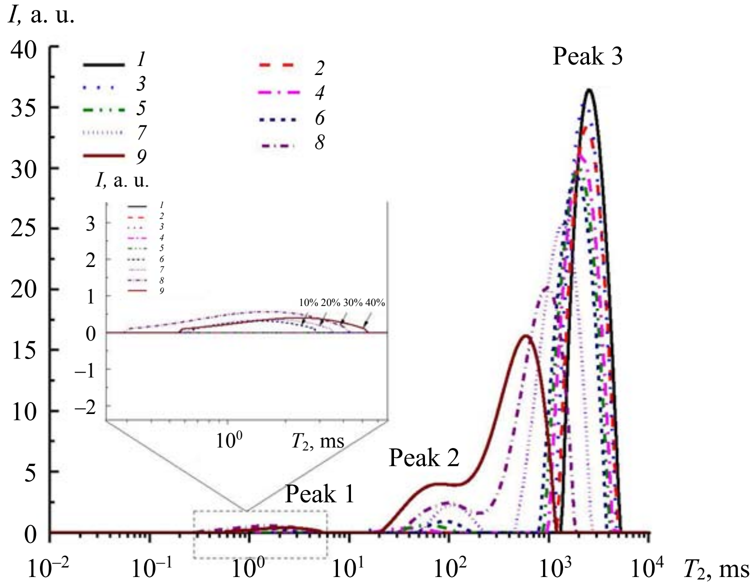

Fig. 1. Transverse relaxation time distribution of the PCE-water solution (PCE-AA5) with concentration of 0 (*1*), 2 (*2*), 4 (*3*), 6 (*4*), 8 (*5*), 10 (*6*), 20 (*7*), 30 (*8*), and 40% (*9*) (the inset is the enlarged image of the peaks with $T_2 < 10$ ms).

It can be seen in Fig. 1 that the sample without PCEs (the PCEs-AA5-0%) has only one T_2 peak (ranging from 1000 to 10000 ms), while the samples with PCEs have three T_2 peaks. The peaks (peak 1) are located between 0.2 and 10 ms and believed to be generated from the water attached on the PCE molecules. However, these T_2 peaks can only be found for the PCE solution whose concentration is higher than 10%. Another two T_2 peaks, peaks 2 and 3, which may result from the water inside the PCE molecules body and the water between PCE molecules, respectively, can also be found in Fig. 1. We can see that peaks 2 and 3 are overlapped in the case of PCEs-AA5 40% and PCEs-AA5 30%. The possible reason for this is that PCE molecules have entanglement (Fig. 2) because the main and side chains of PCE molecules are close when the concentration is high. As a result, the water in the entanglement of PCE molecules would generate a transition zone between the two peaks. It is also found that peak 3 is gradually shifted to the right (bigger T_2 value) as the concentration of PCEs decreases from 40 to 0%.

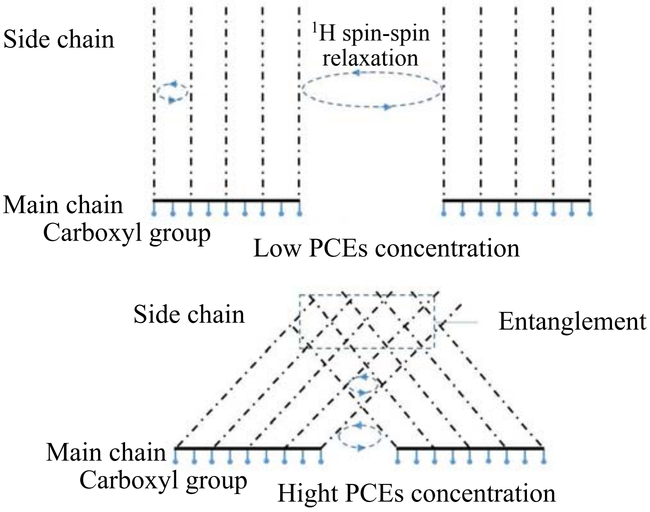

Fig. 2. Diagram of the PCE molecules for low and high PCE concentration.

Relationship between the T_2 value and the PCEs concentration. Here we investigated the relationship between the T_2 values of peak 3 and the concentration of different types of the synthesized PCEs. The T_2 values are expressed as the weighted mean value of T_2 and the relative amplitude

$$T_{2,w} = \sum_{T_{2,\min}}^{T_{2,\max}} \left((T_{2,i}) \frac{A_i}{A_{\text{total}}} \right), \qquad (2)$$

where $T_{2,w}$ is the weighted mean value, $T_{2,i}$ is the transverse relaxation time at the measurement i, A_i is the relative amplitude for the measurement I, and A_{total} is the total amplitude of the T_2 peak. The results in Fig. 3 shows that the T_2 values are linearly correlated with PCE concentrations from 0 to 40% (the fitting results are summarized in Table 2), and their linearity is up to 0.98. This confirms that the low-field NMR method could be an alternative method for the determination of the PCE concentration. Also, it should be noted that the slope of the concentration against the T_2 value is dependent on the PCE type. The slope values (absolute value) increase with the average molecular weight (M_w) of the PCEs.

TABLE 2. The Fitting Results of the T_2 Relaxation Time and Concentration of the PCE-water Solution, Fitting Equation $y = ax + b$

PCEs types	Slope	Intercept	Standard error
AA3	$-1.982 \cdot 10^{-4}$	0.527	0.01205
AA4	$-1.836 \cdot 10^{-4}$	0.480	0.01243
AA5	$-1.805 \cdot 10^{-4}$	0.463	0.01764
AA2-AM	$-1.913 \cdot 10^{-4}$	0.499	0.01243
AA2-AMPS	$-1.914 \cdot 10^{-4}$	0.493	0.01383

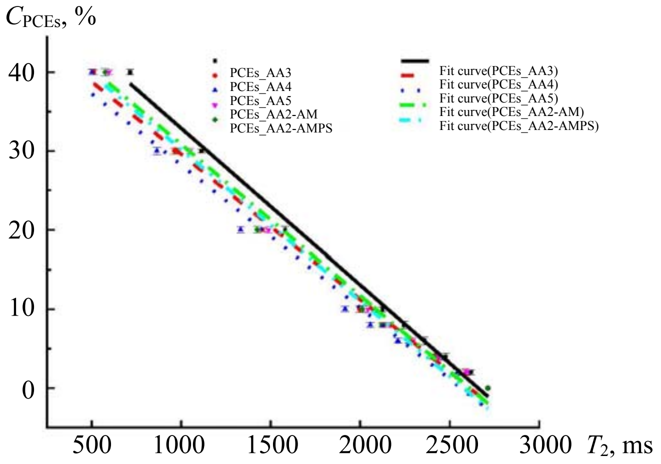

Fig. 3. Relationship between T_2 relaxation time measured by the low-field NMR and PCE concentration from 0 to 40% (error bars are placed to indicate the standard for the concentration).

The relationship between the T_2 value and the molecules weight. The peaks between 0.2 and 10 ms shown in Fig. 1 are believed to be the signals originating from the water attached on the PCE molecules. Thus, theoretically the signal intensity of peak 1 may correlate with the surface of the PCEs molecules in the solutions. Figure 4 shows the relationship between the signal intensity of peak 1 and the average molecular weight of the PCEs molecules. It can be seen that the signal intensity of peak 1 is linearly correlated with the average molecular weight of PCEs molecules when the PCEs concentrations are below 20%. The linearly dependent coefficients for the PCEs concentrations of 10 and 20% are 0.543 and 0.985, respectively. However, there are no obvious correlations between the signal intensity of peak 1 and the molecular weight of PCEs when the concentration is higher than 30%. The possible reason for this outcome is that the high concentration of PCEs may not only create water between the PCE molecules (related to peak 3) but also generate the signals whose T_2 values range from 0.2 to 10 ms, which may interfere with the water signals (related to peak 1) absorbed on the PCEs molecules. Therefore, lower linearity is found for the PCEs with high concentrations.

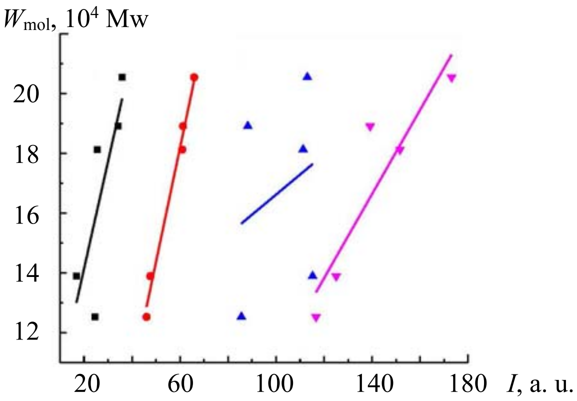

Fig. 4. Relationship between the signal intensity of the peak 1 measured by the low-field NMR and average molecular weight of PCE molecules (the PCE concentration is 10 (■), 20 (●), 30 (▲), and 40% (▼); $R_1^2 = 0.543$, $R_2^2 = 0.985$.

Conclusions. The results evidenced showed that three T_2 peaks could be observed for the PCE-water solution compared with the sample without PCEs. It is found that the T_2 peaks are gradually shifted to the right as the concentration of PCEs decreases from 40 to 0%. The T_2 values are linearly correlated with the PCE concentrations from 0 to 40%, and their linearity is up to 0.98. Moreover, the signal intensity of the T_2 peaks is linearly correlated with the average molecular weight of PCEs molecules when the PCEs concentration is below 20%.

Acknowledgements. The authors acknowledge the financial support provided by the China National Key R&D Program during the 13th Five-year Plan Period (Grant No. 2016YFC0701004), the National Natural Science Foundation of China (Grant No.51678441), the Science and Technology Commission of the Shanghai Municipality (Grant No. 19DZ1202702 and 19DZ1201404), and the Key Science and Technology Foundation of the Gansu Province (Grant No. 19YF3GA004). Gratitude is extended for support from the Shanghai Post-doctoral Excellence Program (2019-2020) and Visiting Scientist project in the Darcy Center of TU/e (2019-2020), the project of 'High-level Foreign Experts' in Tongji University, and the China Scholarship Council. We also like to thank Niumag Electric Corporation (Shanghai, China) for their assistance in performing these measurements.

REFERENCES

1. J. Plank, E. Sakai, C. W. Miao, C. Yu, J. X. Hong, *Cem. Concr. Res.*, **78**, 81–99 (2015).
2. Y. Yu, J. Liu, Q. Ran, et al., *J. Therm. Anal. Calorim.*, **111**, 437–444 (2013).
3. Z. Zhang, Z. Wang, J. Ren, J. Pei, *Iran. Polym. J.*, **25**, No. 6, 549–557 (2016).
4. S. Qian, Y. Yao, Z. Wang, et al., *Constr. Build Mater.*, **169**, 452–461 (2018).
5. H. Yan, Z. Xiong, S. Yaning, et al., *J. Wuhan Univ. Technol. Mater. Sci.*, **33**, No. 4, 932–937 (2018).
6. Y. Qian, K. Lesage, K. E. Cheikh, G. D. Schutter, *Cem. Concr. Res.*, **107**, 75–84 (2018).
7. H. Yan, Z. Xiong, S. Lianglinag, et al., *Constr. Build. Mater.*, **202**, 656–668 (2019).
8. K. Yamada, T. Takahashi, S. Hanehara, et al., *Cem. Concr. Res.*, **30**, No. 2, 197–207 (2000).
9. Y. R. Zhang, X. M. Kong, Z. B. Lu, et al., *Cem. Concr. Res.*, **67**, 184–196 (2015).
10. X. Q. Qiu, X. Y. Peng, C. H. Yi, Y. H. Deng, *J. Disp. Sci. Technol.*, **32**, No. 2, 203–212 (2011).
11. K. R. Brownstein, C. E. Tarr, *Phys. Rev. A*, **19**, 2446–2453 (1979).
12. M. Brax, M. Köhne, E. Kroener et al., *Geoderma*, **340**, 269–278 (2019).
13. Y. J. Yuan, R. Z. Rezaee, M. Verrall, et al., *Int. J. Coal Geol.*, **194**, 11–21 (2018).
14. Y. Ji, Z. Sun, J. Yang, P. Leo, et al., *Constr. Build. Mater.*, **240**, 117938, ISSN 0950-0618 (2020).
15. Y. Ji, P. Leo, Z. Sun, *Cem. Concr. Res.*, **125**, 105866, ISSN 0008-8846 (2019).
16. Lúcio L. Barbosa, Flávio V. C. Kock, et al., *Energy Fuels*, **27**, No. 2, 673–679 (2013).
17. F. C. Giovanna, C. S. Renzo, L. B. Lúcio, et al., *Fuel*, **140**, No. 15, 762–769 (2015).
18. L. Luetkmeyer, B. T. Maria Inês, et al., *Macromol. Symp.*, **258**, No. 1, 108–112 (2007).
19. Y. Ji, Z. Sun, et al., *Constr. Build. Mater.*, **100**, 255–261 (2015).
20. C. Pathama, C. Pavinee, S. Klanarong, et al., *Carbohydr. Polym.*, **53**, No. 3, 233–240 (2015).